Zitierweise: *Angew. Chem. Int. Ed.* **2024**, *63*, e202315917
doi.org/10.1002/anie.202315917

Electrocatalysis

Attenuating *N*-Oxyl Decomposition for Improved Hydrogen Atom Transfer Catalysts

Cheng Yang, Luke A. Farmer, Elvis C. McFee, Rahul Kant Jha, Stephen Maldonado, Derek A. Pratt,* and Corey R. J. Stephenson**

Abstract: The design of *N*-oxyl hydrogen atom transfer catalysts has proven challenging to date. Previous efforts have focused on the functionalization of the archetype, phthalimide-*N*-oxyl. Driven in part by the limited options for modification of this structure, this strategy has provided only modest improvements in reactivity and/or solubility. Our previous mechanistic efforts suggested that while the electron-withdrawing carbonyls of the phthalimide are necessary to maximize the O–H bond dissociation enthalpy of the HAT product hydroxylamine and overall reaction thermodynamics, they undergo nucleophilic substitution leading to catalyst decomposition. In an attempt to minimize this vulnerability, we report the characterization of *N*-oxyl catalysts wherein the aryl ring in PINO is replaced with the combination of a substituted heteroatom and quaternary carbon. By rendering one carbonyl carbon less electrophilic and the other less sterically accessible, the corresponding N^1-aryl-hydantoin-N^3-oxyl radical showed significantly higher stability than PINO as well as a modest improvement in reactivity. This proof-of-principle in new scaffold design may accelerate future HAT catalyst discovery and development.

Introduction

Phthalimide-*N*-oxyl (PINO) is commonly employed as an oxidation catalyst through the facilitation of hydrogen atom transfer (HAT) reactions (Figure 1A).[1] Unlike the ubiquitous persistent nitroxide (2,2,6,6-tetramethylpiperidin-1-yl)oxyl (TEMPO), PINO can readily abstract H-atoms from benzylic and allylic substrates. This difference is a result of the relatively large O–H bond dissociation enthalpy (BDE) of the hydroxylamine of PINO, *N*-hydroxyphthalimide (NHPI, 88 kcal mol^{-1}) relative to the BDE of TEMPO–H (70 kcal mol^{-1}).[2] To this end, PINO has been used for selective electrochemical oxidation of native lignin, stimulating interest in the design of even more potent HAT catalysts.[3]

Previous efforts to design improved *N*-oxyl HAT catalysts have focused on functionalization of the archetype phthalimide motif.[4] However, these modifications tend to manifest improvements either to reactivity *or* to catalyst stability, but not both simultaneously.[4] For example, tetrachloro-PINO, has improved reactivity compared to PINO, but has markedly poorer stability.[5] In contrast, tetraphenyl-PINO has increased stability, apparently due to a fortuitous steric effect, but the HAT reactivity is

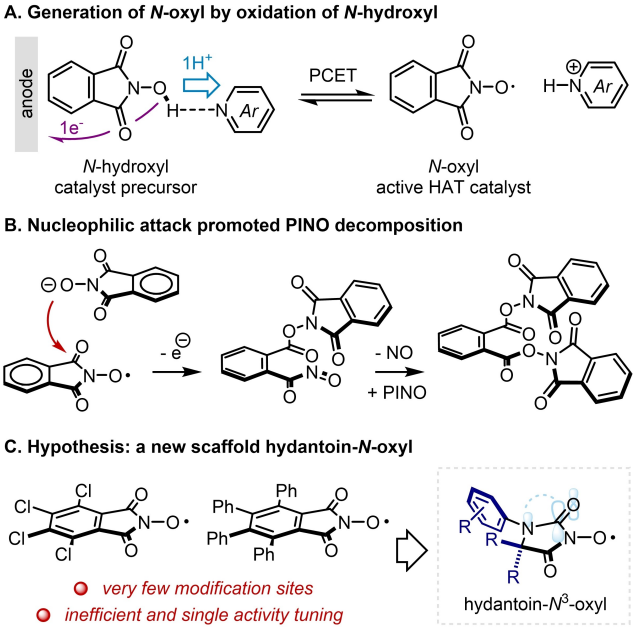


Figure 1. Development of *N*-oxyl hydrogen atom transfer catalysts.

[*] C. Yang, E. C. McFee, R. K. Jha, S. Maldonado, C. R. J. Stephenson
Willard Henry Dow Laboratory, Department of Chemistry, University of Michigan, 930 North University Avenue, Ann Arbor, Michigan 48109, United States
E-mail: smald@umich.edu
crjsteph@umich.edu

L. A. Farmer, D. A. Pratt
Department of Chemistry and Biomolecular Sciences, University of Ottawa, Ottawa, ON K1N 6N5, Canada
E-mail: dpratt@uottawa.ca

S. Maldonado
Program in Applied Physics, University of Michigan, Ann Arbor, Michigan 48109, United States

© 2024 The Authors. Angewandte Chemie published by Wiley-VCH GmbH. This is an open access article under the terms of the Creative Commons Attribution Non-Commercial NoDerivs License, which permits use and distribution in any medium, provided the original work is properly cited, the use is non-commercial and no modifications or adaptations are made.

© 2024 The Authors. Angewandte Chemie published by Wiley-VCH GmbH

negatively affected.[6] Given the opposing relationship between catalyst reactivity and stability, coupled with the well-trodden strategy of manipulating functional groups on NHPI/PINO employed to date, we were motivated to break the mold, so to speak, and explore new molecular scaffolds.

Our recent mechanistic investigations of PINO-catalyzed electrochemical oxidations offered a new point of view on the design of improved HAT catalysts. Although Masui identified a trimeric species as the major decomposition product of PINO in 1987 (Figure 1B), the mechanism of its formation was the subject of wide speculation.[7] Our data suggested that PINO decomposition was initiated by nucleophilic attack of the conjugate base of NHPI on a PINO carbonyl (Figure 1B).[8] This mechanistic insight suggested that electron-withdrawing polarization—a promising way to improve reactivity[5]—would further exacerbate the issue of stability. Reactivity and stability must be considered in concert when designing *N*-oxyl HAT catalysts.

With these considerations in mind, we hypothesized that a more stable *N*-oxyl catalyst that simultaneously retains high HAT reactivity may be obtained by rendering one of the carbonyls *less* electrophilic. A hydantoin-N^3-oxyl (HNO) core structure that features an alternative amide functionality (Figure 1C) fit our design criteria and subsequently became a scaffold of interest. The less electrophilic carbonyl in the amide substituent potentially decreases the propensity for nucleophilic substitution. However, the N^3-hydroxy group, still situated between two carbonyl groups, may retain a sufficiently large O–H BDE to engage in HAT reactions of interest. The broad synthetic accessibility of this structure allows the generation of a large variety of *N*-oxyl compounds, facilitating catalyst discovery. Herein, this report document the evaluation of 14 HNOs representing a wide range of diversity in electronic and steric features as HAT catalysts. The data obtained on the reactivity and stability of these derivatives validate our design strategy and provide an encouraging first step in the development of new *N*-oxyl HAT catalysts.

Results and Discussion

The development of *N*-oxyl catalysts first relies on preparation of their corresponding *N*-hydroxyl precursors.[9] Multiple synthetic methods to access N^3-hydroxyhydantoin (NHH) catalyst precursors were investigated (Figure 2). All N^1-alkylated derivatives and some electron-rich N^1-arylated derivatives were prepared by combining phenyl *N*-hydroxycarbmate and their corresponding *β*-aminoester hydrogen chloride salts in tetrahydrofuran under microwave irradiation.[10] Most N^1-arylated analogues, in particular those derivatives bearing electron-deficient substituents, were synthesized by an aza-oxyallyl cation promoted (hetero)aryl-*N*-alkylation[11] followed by cyclization and deprotection steps. An alternative method to assemble these molecules relied on a Bucherer–Bergs type reaction[12] and subsequent cyclization mediated by CuI.[13] All three synthetic methods were found to be scalable to at least gram-scale (see details in SI).

Our initial evaluation of NHH/HNO focused on the kinetics of C–H abstraction. The rate constant for HAT (k_{HAT}) between the *N*-oxyl species and a model substrate (1-phenylethanol) was estimated through cyclic voltammetric titration.[15] When using PINO as the HAT catalyst, the catalytic current showed a first-order dependence on the concentration of 1-phenylethanol, with k_{HAT} equal to 24.3 $M^{-1}s^{-1}$ at room temperature in MeCN (Figure 3A). The

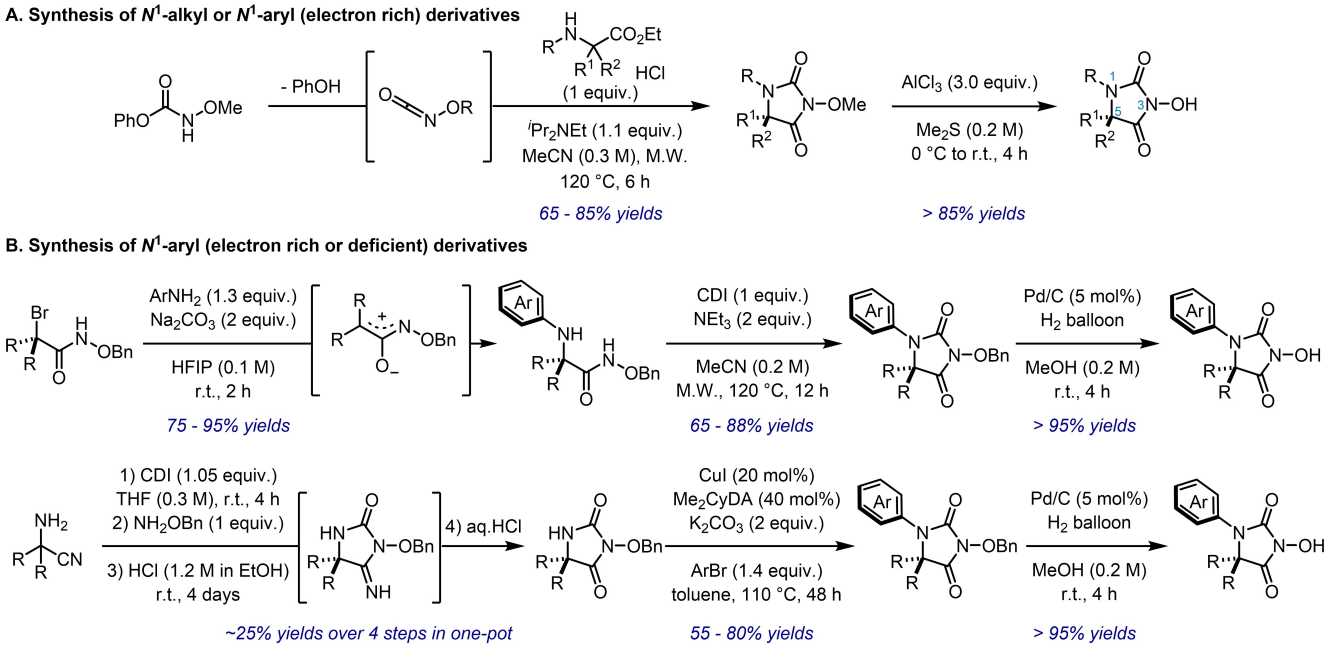


Figure 2. Synthesis of *N*-hydroxyhydantoins.

© 2024 The Authors. Angewandte Chemie published by Wiley-VCH GmbH

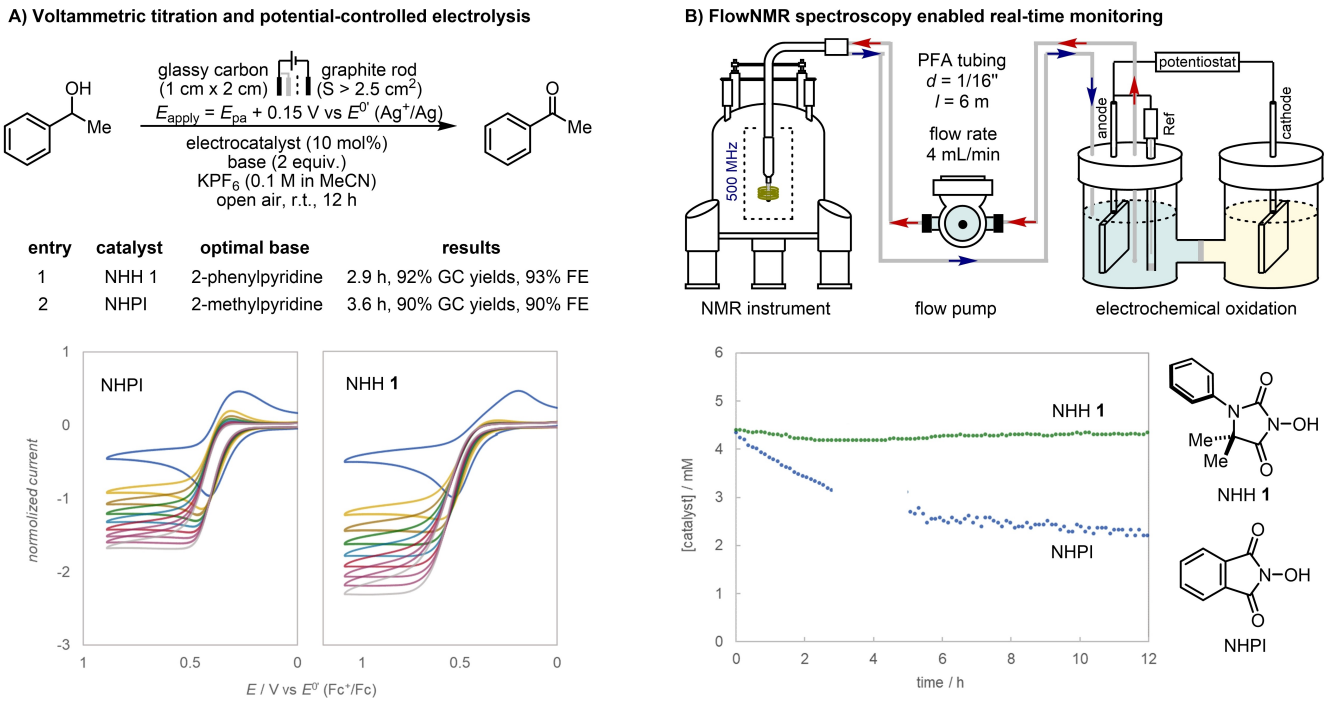


Figure 3. Evaluations of NHH **1** and NHPI as *N*-oxyl catalyst precursors under potential-controlled conditions (cyclic voltammetry to determine k_{HAT}, FlowNMR spectroscopy to determine R_{decay} and bulk electrolysis tounderstand catalytic performance). A) In voltammetry experiments,1-phenylethanol (20 mM, 40 mM, 60 mM, 80 mM, 100 mM) was added to a solution of *N*-hydroxy compounds (2 mM), pyridine (0.2 M), $TBAPF_6$ (0.2 M) in MeCN (5 mL) and the voltammetry was performed at 0.1 Vs-1. FE = Faraday Efficiency. B) In NMR experiments, the catalyst precursor was determined relative to the internal standard 1,3,5-trimethoxybenzene, which is redox-inactive within the investigated potential range,. The reaction solution continuously flowed through the NMR instrument at the rate of 4 mL min^{-1} by an external pump. Relaxation delay was set at 20s to ensure high spectral sensitivity. The missing data points in the NHPI trace is due to the presence of overlapping signals.

measured k_{HAT} between NHO **1** and 1-phenylethanol was 51.0 $M^{-1}s^{-1}$ (Figure 3A).

Satisfied that the HNO scaffold performed comparably to PINO, we were keenly interested in the catalysts' stability. We integrated our electrochemical setup with FlowNMR spectroscopy to perform quantitative, time-dependent monitoring of reaction progress (Figure 3B, see Supporting Information for details).[14] In these measurements, *N*-oxyl precursors NHH and NHPI (4.3 mM in MeCN) were oxidized using a glassy carbon anode in an electrolyte solution containing 5 equiv. of 2,6-lutidine. All bulk electrolysis experiments were conducted at a potential of 0.3 V more positive than the anodic peak potential (E_{pa}) of the *N*-oxyl precursors, which had been measured by cyclic voltammetry at a scan rate of 0.1 Vs^{-1} prior to the reaction. This approach afforded a consistent reaction driving force, enabling head-to-head comparisons of *N*-oxyl stability. The consumption of *N*-hydroxy species provided a surrogate measurement for the decay of the *N*-oxyls. For NHPI, the initial rate of decay (from 20 data points) was measured to be $R_{decay} = 0.03\ M^{-1}s^{-1}$ (Figure 3B). Comparatively, the concentration of NHH **1** remained essentially constant throughout the 12-hour electrolysis and was characterized by a much smaller initial decay rate ($R_{decay} = 0.005\ Ms^{-1}$) compared to NHPI (Figure 3B).

Next, screening of commercially-available bases was performed to evaluate and optimize the catalytic performance of electrochemical oxidation using 1-phenylethanol as a model substrate (see Supporting Information). All reactions were conducted in a divided cell configuration to eliminate the influence of cathodic electrode reactions. Potential-controlled electrolysis was utilized to ensure head-to-head comparison. A potential of +0.15 V beyond E_{pa} was applied to the different NHH/base combinations. A variety of bases spanning ~15 pK_a units were investigated. 2-Phenylpyridine —a slightly weaker base than pyridine[17]—was identified as the optimal base for NHH **1**. With 2-phenylpyridine, the reaction was complete in just 2.9 h with a 92 % yield based upon gas chromatography–mass spectrometry (GC-MS) analysis. All other bases showed current density decreases at the beginning of the reaction (see Supporting Information). It seems that an as yet unidentified base effect plays a role in these rapid current decays. In comparison, NHPI showed the best catalytic performance when using 2-methylpyridine as the base, but required a longer time to afford a similar yield (90 %, 3.6 h). Overall, these results suggested that NHO can promote benzylic alcohol oxidation more efficiently than PINO.

To provide insight on NHO's promising reactivity and establish clear structure–reactivity relationships, we evaluated the reactivity and stability of a variety of other NHO analogs (Figure 4). The decreased stability of NHH **2** suggested that it was important to protect the C5 position in the hydantoin core. Both N^1-methylated NHH **3** and bicyclic

© 2024 The Authors. Angewandte Chemie published by Wiley-VCH GmbH

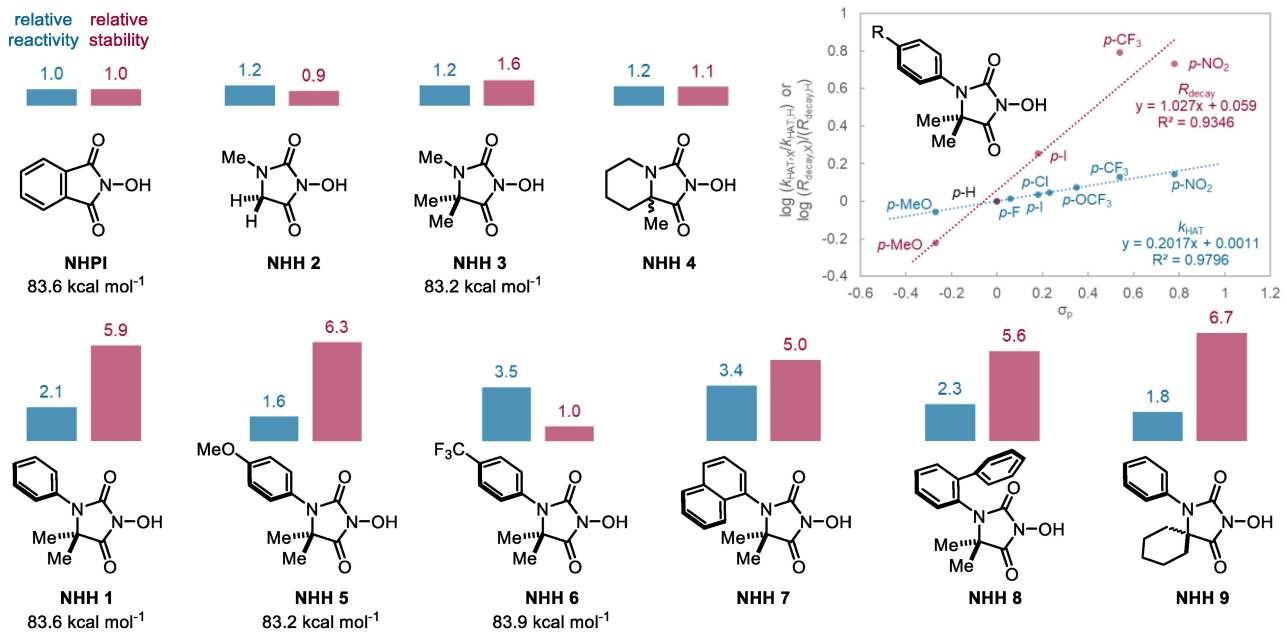


Figure 4. Evaluation of a set of 14 N3-hydroxyhydantoins as potential HAT mediators. Relative reactivity and stability were determined using cyclic voltammetric titration and FlowNMR spectroscopy, respectively, as in Figure 3. The k_{HAT} (with 1-phenylethanol) and R_{decay} of NHPI were both arbitrarily set to 1 and all other results are reported as relative values. O-H BDEs were calculated using CBS-QB3.

NHH **4** showed only modest improvement in stability and reactivity. Compared to these alkylated NHH species, the phenyl group on the N^1 site was critical to maintain desired reactivity and stability. To better understand the reactivity trends, we carried out CBS-QB3 calculations[18] on several derivatives to predict their O–H BDEs. The O–H BDEs of NHH **1** and NHH **3** were predicted to be 83.5 and 83.2 kcal mol^{-1}, respectively—both essentially indistinguishable from the calculated value for NHPI (83.6 kcal mol^{-1}) and therefore consistent with the similar k_{HAT} determined for these *N*-oxyl species. The introduction of steric hindrance at N^1 (e.g., naphthalene, NHH **7**; 2,2'-biphenyl, NHH **8**) or C5 (cyclohexyl, NHH **9**) did not impart significant improvement on the stability or considerable impact on k_{HAT}.

Given the higher stability of NHH **1**, the degree to which the reactivity could be tuned by changing the substituents on the N^1-phenyl moiety was assessed. Linear free energy relationships were obtained for both k_{HAT} and R_{decay} using *para*-substituted derivatives of NHH **1** (Figure 4). The logarithm of their decay rates relative to that measured with H (i.e., $\log(R_{decay,X}/R_{decay,H})$) were found to correlate with σ_p values[16] ($R^2 = 0.93$) with a reaction constant $\rho = 1.03$. A corresponding correlation with the HAT kinetics yielded a smaller $\rho = 0.20$ as determined from an even more robust correlation ($R^2 = 0.98$). The presence of an electron-donating group (OMe, NHH **5**) or an electron-withdrawing group (CF_3, NHH **6**) on the 4-position of the phenyl substituent was predicted to have a marginal effect on the O–H BDEs, with values of 83.2 and 83.9 kcal mol^{-1}, respectively, but are nonetheless consistent with the modest changes in k_{HAT} determined by experiment and the modest slope depicted in the Hammett plot (Figure 4). Overall, it is clear that 1) electron-donating groups (EDGs) can increase catalyst stability while modestly decreasing the reactivity, and 2) electron-withdrawing groups (EWGs) can modestly improve the reactivity but sharply decrease catalyst stability.

In a bid to understand the decay process of the NHH-type catalyst, product analysis of NHO decomposition (NHO **6**) was carried out. Following electrolysis of NHH **6** (4-CF_3) in the presence of 2,4,6-collidine for 4 h, its corresponding hydantoin—resulting from deoxygenation—was isolated as the major product (**SI**). In contrast to NHPI,[8] when using high-resolution mass spectrometry to analyze the final reaction solution, neither ring-opened trimer nor dimer were observed. Although the decomposition of NHH/HNO **6** clearly follows a distinct path from that of NHPI/PINO, the mechanism of deoxygenation leading to the observed product is unclear.[19]

The steric effects on the rate of HAT was also investigated. Several benzylic alcohols were chosen as model substrates. When using NHPI as a mediator, steric effects on the HAT rate were considerable (Table 1). Compared to 1-phenylethanol, the k_{HAT} of benzyl alcohol increased by ~50 %. Substitution on the 2-, 6- or α- positions led to a marked decrease in the HAT reactivity. The reactivity oft he NHH species showed similar trends. Tuning the electronics of NHH did not yield a change in the HAT reactivity pattern.

Given its key role in the reaction, an NHO radical and its decay by electron paramagnetic resonance (EPR) was characterized. NHO **1** was generated by irradiation of an argon-saturated solution of NHH **1** (20 mM) and 10 % v/v di-*tert*-butyl peroxide (DTBP) in benzene using a Hg-vapor

© 2024 The Authors. Angewandte Chemie published by Wiley-VCH GmbH

Table 1: Steric effects on HNO-catalyzed HAT. Rate constants are given relative to k_{HAT} between NHPI and 1-phenylethanol.

catalyst	substrate	k_{HAT}[a]
NHPI	1-phenylethanol	1
	benzyl alcohol	1.5
	α,2,6-Trimethylbenzenemethanol	<0.5
	α-(1,1-Dimethylethyl)benzenemethanol	<0.5
NHH1	1-phenylethanol	2.1
	benzyl alcohol	3.1
	α,2,6-Trimethylbenzenemethanol	<0.5
	α-(1,1-Dimethylethyl)benzenemethanol	<0.5
NHH5	1-phenylethanol	1.6
	benzyl alcohol	2.0
	α,2,6-Trimethylbenzenemethanol	<0.5
	α-(1,1-Dimethylethyl)benzenemethanol	<0.5
NHH6	1-phenylethanol	3.4
	benzyl alcohol	4.5
	α,2,6-Trimethylbenzenemethanol	<0.6
	α-(1,1-Dimethylethyl)benzenemethanol	<0.5

lamp in the cavity of an EPR spectrometer (top of Figure 5A). The characteristic *g*-factor ($g=2.0074$) was similar to what was previously reported for PINO ($g=2.0070$),[7] but the hyperfine coupling pattern featured a triplet of triplets for the ^{14}N of the *N*-oxyl ($\alpha_N^a=3.90$ G) and *N*-phenyl ($\alpha_N^b=1.23$ G), respectively. Hyperfine coupling constants and the isotropic *g*-factor predicted from the spin density matrix of a B3LYP/EPR-III calculation yielded a very similar simulated spectrum (bottom of Figure 5A). It is important to note that neither the experimental nor the simulated EPR show any discernable hyperfine couplings from the protons on the phenyl substituent, indicating negligible delocalization of the unpaired electron by the aromatic ring. This is fully consistent with the computed isosurface depicting the spin density distribution in HNO **1** (Figure 5B), where it is apparent that the spin density is greatest on the *N*-oxyl moiety, with a modest degree of delocalization across the other heteroatoms of the hydantoin core. The lack of spin distribution on the phenyl moiety results from the lack of conjugation between the phenyl and hydantoin rings, which are almost perpendicular in the minimum energy structure ($\theta=79°$). This aspect accounts for the minimal electronic substituent effects on k_{HAT} and the computed O–H BDEs in Figure 4. By eliminating the resonance contributions of the substituents, only the modest inductive effects remain.

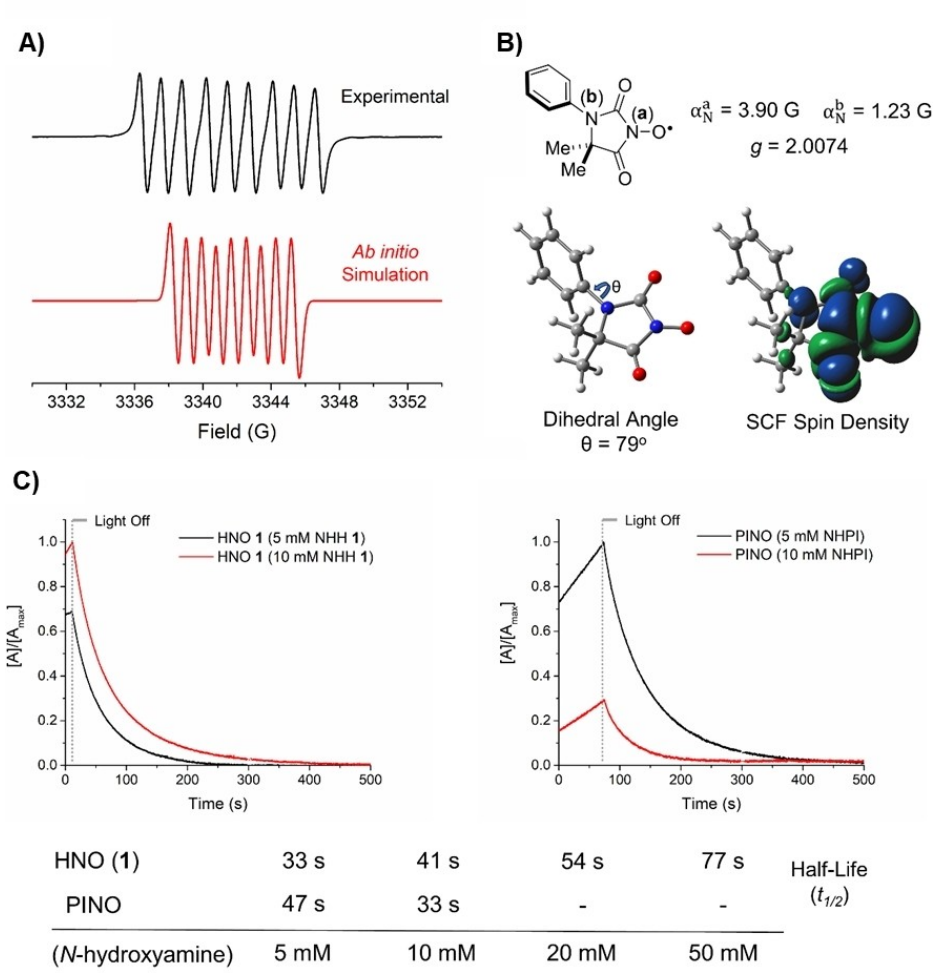
We further sought insight to the persistence of HNO **1** and examined its decay using static-field-time-sweep kinetic EPR. Photolysis in the presence of peroxide as above (except that acetonitrile was used in lieu of benzene) for 15–50s led to a modest accumulation of HNO **1** that was dependent on the starting concentration of NHH. Removal of the light source was accompanied by a rapid first-order decay in the signal (e.g., Figure 5C and S3). At higher concentrations of NHH **1**, the nitroxide appeared to be slightly more persistent possibly indicating that the NHH could have a stabilizing effect on the nitroxide, possibly via H-bond formation between the *N*-oxyl and *N*-hydroxy moieties of HNO **1** and NHH **1**, respectively (i.e., NO•–H–NO).[20]

In a bid to compare the persistence of HNO **1** to PINO under the same conditions, we conducted analogous experiments using NHPI in lieu of NHH **1**. Generation of PINO required substantially longer periods of irradiation (4–7 min) to accumulate sufficient signal to obtain reproducible decay traces. In stark contrast to the observations made with HNO/NHH, the accumulation of PINO was attenuated on going from 5 to 10 mM NHPI. At higher concentrations of NHPI (≥ 20 mM), no PINO could be detected—even upon increasing the irradiation time. The decay of PINO, like HNO, followed good first-order kinetics, but in contrast to HNO, PINO was less persistent when NHPI concentration was increased. This observation is consistent with the premise that NHPI reacts at a carbonyl carbon of PINO to drive decomposition.[8] The contrasting behavior of NHPI/PINO and NHH/HNO indicates that the decomposition of HNO is mechanistically distinct from that of PINO. Although HNO is similarly persistent to PINO under the present conditions, this may not be the case during the electrocatalytic reactions, where these radicals may have a much higher steady-state concentration and where the non-nucleophilic bases used to facilitate the electrochemical oxidation can catalyze PINO decomposition via the reaction of the conjugate base of NHPI with PINO.

Hydantoin-*N*-oxyl is a new scaffold that possesses promising HAT performance when compared to canonical phthalimide-derived catalysts. Our results demonstrate that *N*-oxyl persistence can be increased without sacrificing reactivity. To the best of our knowledge, this is the first design of PINO-type catalysts that demonstrates concurrent improvements in both reactivity and stability. The presented data indicate that rendering one carbonyl less electrophilic measurably increases the persistence of the *N*-oxyl. The change of the major decomposition product—from trimer to deoxygenation species—is consistent with the premise that adjacent nitrogen altered the nucleophilic attack mechanism, the predominant decay path of PINO. These results were both in line with the nucleophilic decay path being relevant to the lifetime of PINO[8] and consistent with our hypothesis of making the carbonyl less electrophilic to be an important catalyst design approach.

The design of NHO catalysts opens up new opportunities for further HAT catalyst discovery. First, the decomposition mechanism of NHO should be understood to further improve *N*-oxyl persistence. Since no other products were observed and mass recovery exceeded 90 %, we propose that oxygen atom abstraction from the electrode surface is responsible. Detailed analysis of the carbon electrode may provide mechanistic insights. Second, deconvolution of the complicated base effect associated with NHO may lead to a better catalyst with higher base compatibility. Third, this proof-of-principle study focused on a limited number of candidates; further derivatization/optimization of the NHO scaffold certainly merits further investigation. Fourth, other heteroatoms should be explored to expand the current adjacent atom effect as similar structures bearing other heteroatoms may possess further improved activities.

© 2024 The Authors. Angewandte Chemie published by Wiley-VCH GmbH



HNO (**1**)	33 s	41 s	54 s	77 s	Half-Life ($t_{1/2}$)
PINO	47 s	33 s	-	-	
(*N*-hydroxyamine)	5 mM	10 mM	20 mM	50 mM	

Figure 5. A) Experimental (20 mM of NHH **1** in benzene containing 10% v/v DTBP under continuous irradiation with light from a low-pressure Hg-vapor lamp) and simulated (B3LYP/EPR-III from the B3LUP/CBSB7 geometry of the CBS-QB3 calculation) EPR spectra of HNO **1**. B) Experimental spectral parameters and computed geometry and spin density of HNO **1**. C) Representative decay traces corresponding to HNO **1** and PINO generated from NHH **1** and NHPI, respectively (5–50 mM hydroxylamine in acetonitrile containing 10% v/v DTBP irradiated by light from a Hg-vapor lamp).

Conclusion

In summary, this paper details an efficient HAT electrocatalyst scaffold: hydantoin-N^3-oxyl. With a nitrogen atom adjacent to one of the carbonyls, the new structures showed significant improvement in stability and modest increase in HAT reactivity. This design is different and potentially more general than previous strategies relying solely on functionalization of the phthalimide core. The data here are collectively a proof-of-concept that multiple parameters can and should be considered comprehensively in the design of more efficient *N*-oxyl-type HAT catalysts.

Supporting Information

Supporting Information including cyclic voltammetry, electrolysis, computational studies, compound characterization. (PDF)

Acknowledgements

C.R.J.S. and S.M. acknowledge the financial support from the National Science Foundation (CBET-2033714), and the University of Michigan. D.A.P. acknowledges the financial support from the Natural Sciences and Engineering Research Council of Canada. This work was enabled by support provided by Compute Ontario and Compute Canada (www.computecanada.ca). C.Y. acknowledges a Rackham pre-doctoral fellowship and a Wirt & Mary Cornwell Award from the University of Michigan.

Conflict of Interest

The authors declare no conflict of interest.

© 2024 The Authors. Angewandte Chemie published by Wiley-VCH GmbH

Data Availability Statement

The data that support the findings of this study are available in the supplementary material of this article.

Keywords: hydrogen atom transfer · electrocatalysis · oxidation · radicals

[1] F. Recupero, C. Punta, *Chem. Rev.* **2007**, *107*, 3800–3842.
[2] R. Amorati, M. Lucarini, V. Mugnaini, G. F. Pedulli, F. Minisci, F. Recupero, F. Fontana, P. Astolfi, L. Greci, *J. Org. Chem.* **2003**, *68*, 1747–1754.
[3] I. Bosque, G. Magallanes, M. Rigoulet, M. D. Kärkäs, C. J. R. Stephenson, *ACS Cent. Sci.* **2017**, *3*, 621–628.
[4] a) C. Yang, S. Arora, S. Maldonado, D. A. Pratt, C. R. J. Stephenson, *Nat. Chem. Rev.* **2023**, *7*, 653–666; b) S. Zhang, M. Findlater, *ACS Catal.* **2023**, *13*, 8731–8751.
[5] Q. Zhang, C. Chen, H. Ma, H. Miao, W. Zhang, Z. Sun, J. Xu, *J. Chem. Technol. Biotechnol.* **2008**, *83*, 1364–1369.
[6] M. Nechab, C. Einhorn, J. Einhorn, *Chem. Commun.* **2004**, 1500–1501.
[7] C. Ueda, M. Noyama, H. Ohmori, M. Masui, *Chem. Pharm. Bull.* **1987**, *35*, 1372–1377.
[8] C. Yang, L. A. Farmer, D. A. Pratt, S. Maldonado, C. R. J. Stephenson, *J. Am. Chem. Soc.* **2021**, *143*, 10324–10332.
[9] In this paper, we use the NHH/HNO abbreviation to represent the redox couple. NHH is the catalyst precursor, while HNO is the active HAT catalyst. NHO = *N*-hydroxyhydantoin; HNO = hydantoin-*N*-oxyl.
[10] R. A. Ivanovich, D. A. Polat, A. M. Beauchemin, *Adv. Synth. Catal.* **2017**, *359*, 4289–4293.
[11] A. J. Ansari, A. Yadav, A. Mukherjee, E. Sathish, K. Nagesh, R. Singh, *Chem. Commun.* **2020**, *56*, 4804–4807.
[12] T. Kurz, D. Geffken, K. Widyan, *Tetrahedron* **2004**, *60*, 2409–2416.
[13] P. Thilmany, P. Gérard, A. Vanoost, C. Deldaele, C. Petit, G. Evano, *J. Org. Chem.* **2019**, *84*, 392–400.
[14] A. M. R. Hall, J. C. Chouler, A. Codina, P. T. Gierth, A. J. Lowe, U. Hintermair, *Catal. Sci. Technol.* **2016**, *6*, 8406–8417.
[15] C. Costentin, J. M. Savéant, *ChemElectroChem* **2014**, *1*, 1226–1236.
[16] C. Hansch, A. Leo, R. W. Taft, *Chem. Rev.* **1991**, *91*, 165–195.
[17] The pK_a of 2-phenylpyridine in MeCN is unknown. This statement is based on an estimation from their bascity in water (2-phenylpyridine = 4.48; pyridine = 5.24). The pK_a values were obtained from the iBond 2.0 data base: http://ibond.nankai.edu.cn/. (Accessed on Jan 11, 2023).
[18] J. A. Montgomery, M. J. Frisch, J. W. Ochterski, G. A. Petersson, *J. Chem. Phys.* **1999**, *110*, 2822–2827.
[19] A similar trend in NHH/HNO base-stability was observed as with NHPI/PINO. As the base becomes stronger, the *N*-oxyl tends to be less stable (less reversible by voltammetry). Similar to PINO, HNO is unstable in basic buffered solutions.
[20] P. Franchi, M. Lucarini, P. Pedrielli, G. F. Pedulli, *ChemPhysChem* **2002**, *3*, 789–793.

Manuscript received: October 20, 2023
Accepted manuscript online: March 4, 2024
Version of record online: April 22, 2024

© 2024 The Authors. Angewandte Chemie published by Wiley-VCH GmbH